The effects of calcium buffering and cyclic AMP on mechano-electrical transduction in turtle auditory hair cells

A. J. Ricci and R. Fettiplace*

Department of Neurophysiology, University of Wisconsin Medical School, Madison, WI 53706, USA

1. The effects of intracellular Ca^{2+} buffering on hair cell mechanotransduction were studied in an intact cochlear epithelium where the endolymphatic and perilymphatic surfaces could be separately perfused with different Ca^{2+} solutions.

2. The speed and extent of transducer adaptation increased as the concentration in the patch electrode of the Ca^{2+} buffer BAPTA was lowered. In 0·1 mM BAPTA or less, the transducer adapted almost completely, with a mean time constant of 0·8 ms.

3. For a fixed internal BAPTA concentration, the transducer conductance varied with hair cell location, increasing towards the high-frequency end of the cochlea, and the time constant of adaptation decreased proportionally. At a given cochlear location, hair cells with larger transducer conductances displayed faster adaptation. We suggest that transducer adaptation accounts for a variable high-pass filter observed in the acoustic tuning curve.

4. The effects of perfusion of 50 μM Ca^{2+} endolymph depended on the BAPTA concentration of the electrode: with 3 mM BAPTA, adaptation was abolished, but in most recordings with 0·01 or 0·1 mM BAPTA, rapid adaptation was retained. The current–displacement curve was also shifted less the lower the intracellular BAPTA concentration. Cells in the high-frequency half of the papilla retained adaptation at a higher BAPTA concentration.

5. Treatment with the cAMP agonist, 8-bromo-cAMP, or with the phosphodiesterase inhibitor 3-isobutyl-1-methylxanthine, caused a rightward shift in the current–displacement curve which was independent of the internal BAPTA concentration.

6. We conclude that the free Ca^{2+} and cyclic nucleotide concentrations of the hair bundle modulate the position of the activation curve of the transducer. The factors which may be important for the correct functioning of adaptation *in vivo* are discussed.

Hair cells are epithelial cells whose transducing surface, the mechanically sensitive hair bundle, is exposed to low-Ca^{2+} endolymph and whose synaptic connections on the basolateral aspect are enveloped in high-Ca^{2+} perilymph. Recent evidence suggests that the mechano-electrical transduction channels are located at either end of extracellular strands linking the distal tip of each stereocilium with the body of its taller neighbour (Denk, Holt, Shepherd & Corey, 1995). Such placement enables the channels to sense the tilting of the stereocilia in a direction parallel to the axis of symmetry of the bundle (Pickles, Comis & Osborne, 1984). An adaptation process has also been described which sets the operating range of the transducer, thus enabling the channels to detect small displacements centred around the ambient position of the stereocilia (Eatock, Corey & Hudspeth, 1987). Adaptation is thought to be triggered by a rise in intracellular Ca^{2+} following influx through the transduction channels (Assad, Hacohen & Corey, 1989; Crawford, Evans & Fettiplace, 1989; Kimitsuki & Ohmori, 1992).

Employing Ca^{2+} as the feedback signal poses a problem since the endolymphatic Ca^{2+} concentration may be as low as 30 μM in mammals (Bosher & Warren, 1978) and 65 μM in turtles (Crawford, Evans & Fettiplace, 1991). Moreover, when isolated hair cells are immersed in solutions containing 20–50 μM Ca^{2+}, transducer adaptation is lost and the channels become more than 50% activated at rest (Crawford *et al.* 1991; Kimitsuki & Ohmori, 1992). This implies that in low-Ca^{2+} endolymph, insufficient Ca^{2+} may be entering the stereocilia through the transduction channels to implement adaptation. One hypothesis is that other intracellular factors exist for determining the efficacy of Ca^{2+} to regulate the degree of activation of the transduction channels and the 'set position' of the hair bundle at rest. To explore this problem further we have measured hair cell transduction

* To whom correspondence should be addressed.

currents in an intact epithelium, where the endolymphatic and perilymphatic surfaces can be separately perfused. Use of the intact papilla has significantly increased the number of successful recordings and has prolonged the recording time, thus enabling a more systematic study of the transduction apparatus in single hair cells. Our results indicate that the degree of Ca^{2+} buffering within the stereocilia is an important factor influencing transducer adaptation. In view of the reports of adenyl cyclase in hair cell stereocilia (Oudar, Ferrary & Feldmann, 1990; Drescher, Kern, Hatfield & Drescher, 1995), and cAMP actions on a hair cell epithelium (Ricci, Norris & Guth, 1991), we have also investigated the involvement of the intracellular messenger in hair cell transduction. These experiments have shown that cAMP may co-operate with Ca^{2+} in setting the activation range of the transducer.

METHODS

Preparation and recording

Turtles (*Trachemys scripta elegans*, carapace length, 100–125 mm) were decapitated and the heads split sagitally with a razor blade. The cochlear duct and lagena (with an attached portion of the saccule) were removed and opened and the tectorial membrane was carefully peeled away following digestion for ~20 min in saline solution (mM: NaCl, 125; KCl, 4; $CaCl_2$, 2·8; $MgCl_2$, 2·2; glucose, 8; NaHepes, 10; pH, 7·6) containing up to 0·1 mg ml^{-1} protease (Sigma Type XXIV). A prerequisite for observing large transduction currents was adequate protease treatment so that the tectorial membrane could be detached without tugging on the hair bundles. The preparation was transferred to a Sylgard well (volume, ~1 ml) in the recording chamber and secured, hair bundles uppermost, with strands of dental floss tensioned on insect pins; the tension could be adjusted so that most of the papilla surface overlying the basilar membrane lay in one focal plane. This portion of the papilla is approximately 800 μm long and 150 μm wide (see Hackney, Fettiplace & Furness, 1993). The chamber was mounted on the stage of a Zeiss Axioskop FS microscope and viewed using Nomarski optics through a ×63 water-immersion objective lens (numerical aperture, 0·9), a ×1·6 optovar and a Hamamatsu C2400 CCD camera. Experiments were performed at 22–24 °C. Results are expressed in the text as means ± 1 standard error of the mean (S.E.M.).

Whole-cell currents were recorded with borosilicate patch electrodes connected to a List EPC-7 amplifier. The first electrode was used to breach the abneural side of the papilla at the level of the cell bodies. This manoeuvre made only a small hole in the side of the papilla and left the apical surface of the hair cells unperturbed. A new recording electrode was then advanced into the track made by the previous penetration, rupturing the connections between the supporting cells to make contact with the basolateral aspect of a hair cell. With successive electrodes, it was possible to record from each hair cell in a row advancing across the papilla towards the neural limb, but usually the first recording was taken from the third cell in from the abneural edge (Fig. 1*B*), leaving the intervening hair cells and supporting cells intact. This precaution ensured that the endolymph solution did not reach the basolateral surface of the hair cell under study (see below). The experimental approach is similar to that used by Kros, Rüsch & Richardson (1992) for recording transduction currents in a mouse cochlea, with the exception that in the present experiments no tissue was removed to gain access to the basolateral surface of the cell (Fig. 1). Recording in the intact papilla has the advantages that, during preparation, the hair bundles are subject to less mechanical disturbance than occurs with isolated hair cells and that there is no enzymatic digestion with papain, which together may account for the larger transduction currents.

Electrodes were filled with a solution of composition (mM): CsCl, 120; Na_2ATP, 3; $MgCl_2$, 3; CsHepes, 10; pH 7·2 and various amounts of the Ca^{2+} buffer Cs_4BAPTA (Molecular Probes, Eugene, OR, USA). BAPTA concentrations of 0·01, 0·1, 0·5, 1, 3 and 10 mM were used, and with the two highest concentrations, the CsCl was reduced to keep the osmolarity constant. The Cs^+-based intracellular solution blocked the large Ca^{2+}-activated K^+ currents present in turtle hair cells. The electrode resistance was 10–15 MΩ and up to 50% series compensation was applied, giving a range of recording time constants from 75 to 225 μs. During the initial phase of a recording, there were changes in the transducer response, which may partly stem from the time course of equilibration of the pipette solution with the cell interior. From the access resistance of the electrodes, it can be estimated (Oliva, Cohen & Mathias, 1988) that the time constant of 'wash-in' for a substance the size of BAPTA is about 2–3 min; for loss of larger cytoplasmic molecules like the purported Ca^{2+} buffer calbindin-28k, 'wash-out' may take somewhat longer. In practice, about 10 min were allowed before acquiring control responses. Transducer currents in response to hair bundle displacement were measured at a holding potential of −70 mV and were stored on a Sony PCM instrumentation recorder at a bandwidth of 0–20 kHz. At the end of a recording the longitudinal position of the hair cell and the total length of the papilla were noted.

Mechanical stimulation

The apparatus for deflecting hair bundles with a stimulator stiffer than the bundle was identical to that previously described (Crawford *et al.* 1989). A rigid borosilicate pipette (tip fire polished to a diameter of about 1 μm) was cemented to a piezoelectric bimorph with displacement sensitivity and resonant frequency of about 0·1 μm V^{-1} and 23 kHz, respectively. During an experiment, the shank of the glass probe was oriented along the long axis of the papilla and its distal end was bent at an angle of ~70 deg. The tip of the probe could then be placed into the rake of the hair bundle to displace the bundle towards or away from the kinocilium. Appropriate positioning of the probe was achieved by advancing the probe onto the hair bundle during delivery of small displacement steps until a response or a baseline deflection was just detectable. The bimorph was driven differentially with voltage steps, filtered with a 4-pole Bessel filter at 6 kHz to minimize excitation of the bimorph resonance, and amplified through a high-voltage driver amplifier of 20-fold gain. This arrangement yielded a fast stimulator with a 10–90% rise time of about 60 μs (Crawford *et al.* 1989). A current–displacement relationship was generated by delivering a family of positive and negative displacement steps (towards and away from the kinocilium, respectively) 20 or 50 ms in duration at a repetition rate no greater than 5 s^{-1}. Each point on the relationship was the mean of five to fifty presentations. Transducer behaviour was characterized with as few stimulus families as possible to avoid run-down in the current amplitude, this being especially important during long recordings such as those with the cAMP analogues (Fig. 9). The unattenuated amplitude of the stimulator was measured at the end of each experiment. The glass probe was acid cleaned at the start of the experiment so that it would adhere to the hair bundle membrane. This ensured that the bundle followed faithfully both positive and negative deflections of the probe.

Perfusion

The preparation was continuously perfused with saline solution of composition (mM): NaCl, 125; KCl, 0·5; $CaCl_2$, 2·8; $MgCl_2$, 2·2; glucose, 8; sodium pyruvate, 2; NaHepes, 10; pH 7·6. The upper (endolymphatic) surface of the hair cells was separately perfused by a large pipette, 100 μm internal diameter, introduced into the cochlear duct, the flow rate being about 10-fold less than the bath perfusion rate. The perfusion pipette was connected to a six-inlet manifold (Warner Instruments, Hamden, CT, USA) fed from a Gilson peristaltic pump, a given inlet being selected by means of a remotely controlled miniature solenoid valve (Lee Products, Westbrook, CT, USA); the time for solution exchange in the duct was about 1 min. Solutions of different Ca^{2+} concentration perfused into the cochlear duct had ionic compositions of (mM): NaCl, 134; KCl, 0·5; $CaCl_2$, 2·8, 0·25 or 0·05; glucose, 8; NaHepes, 10; pH 7·6. The solution with 2·8 mM $CaCl_2$ also contained 2·2 mM $MgCl_2$. It should be stressed that the cochlear duct was continuously perfused throughout the experiment with solutions containing either normal Ca^{2+} (2·8 mM) or low Ca^{2+} (250 or 50 μM). The rate of perfusion of the cochlear duct was minimized both to prevent inadvertent stimulation of the bundles and to localize the stream of solution around the hair bundle being studied. Ca^{2+} concentrations were calibrated using a calcium-sensitive electrode (Microelectrodes Inc., Londonderry, NH, USA).

The effects of low-Ca^{2+} solutions to augment the transduction current and slow adaptation (see below) could be achieved with little or no reduction in the maximum amplitude of the voltage-dependent Ca^{2+} current recorded during the perfusion procedure (Fig. 1). The voltage-dependent Ca^{2+} current was monitored in the majority of experiments, and its peak amplitude was reduced by no

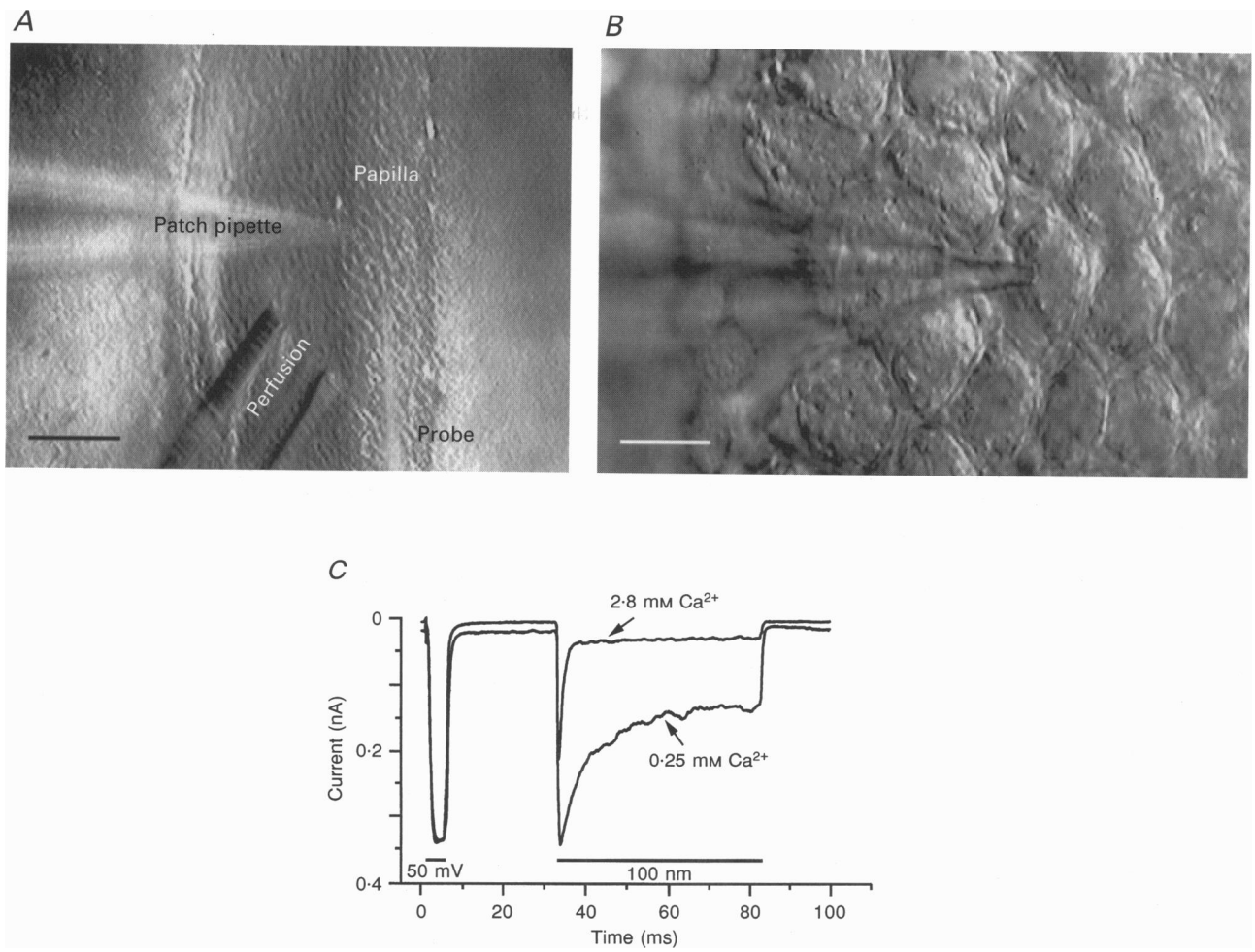

Figure 1. Recording and perfusion arrangements

A, low-power view of the basilar papilla depicting the positions of the recording electrode (Patch pipette), the stimulating probe and the pipette for perfusing the cochlear duct (Perfusion). The patch electrode is introduced through a small hole in the abneural face of the papilla; the lagena is at the top. Scale bar, 100 μm. *B*, high-power view of the papilla with the electrode contacting a hair cell near its base. Note that the cells closer to the abneural edge of the papilla on the left are still intact. Scale bar, 10 μm. *C*, simultaneous recordings of the voltage-dependent Ca^{2+} current and the transducer current. Bars below the records give the timing of a 50 mV depolarizing step and a 100 nm bundle deflection. Superimposed traces during perfusion of the cochlear duct with solutions containing 2·8 and 0·25 mM Ca^{2+} are shown. Note that the augmentation and slowing of the transducer current in the low-Ca^{2+} solution is achieved with no reduction in the Ca^{2+} current. Electrode Ca^{2+} buffer, 0·5 mM BAPTA. Holding potential, −70 mV.

more than 20% on lowering the endolymphatic [Ca^{2+}] to 250 or 50 μM. Since the Ca^{2+} channels are likely to be confined to the basolateral membrane (Roberts, Jacobs & Hudspeth, 1990; Tucker & Fettiplace, 1995), this argues that solutions perfused into the cochlear duct had their major effect on the apical surface of the hair cells, thus mimicking the *in vivo* separation of endolymph and perilymph. The cyclic nucleotide agonist 8-bromo-cAMP (8-Br-cAMP) and the phosphodiesterase inhibitor 3-isobutyl-1-methylxanthine (IBMX), which in some experiments were also included in the cochlear duct perfusate, were obtained from Calbiochem (San Diego, CA, USA).

RESULTS

The effects of Ca^{2+} buffers on transduction currents

The transduction current measured in the intact papilla in response to stepping the bundle activated rapidly in less than 0·5 ms but was then terminated by an adaptation that returned the current towards its original resting level. These features, illustrated in Fig. 2 for endolymph solution containing 2·8 mM Ca^{2+}, resemble qualitatively those reported for isolated turtle hair cells (Crawford *et al.* 1989). The characteristics of adaptation for a small response were strongly influenced by the amount of Ca^{2+} buffer in the electrode solution (Figs 2 and 3). With 3–10 mM BAPTA, adaptation was slowed or abolished (Crawford *et al.* 1989), whereas with low concentrations of 0·01–0·1 mM BAPTA, the current adapted almost completely with a time constant under 1 ms. Figure 2*D* shows the relationship between the transducer current I, normalized to its peak value I_{max}, and bundle displacement, x, for the three different cells. The plots suggest that with reduced BAPTA concentration a smaller fraction of the current is activated at rest, and the transducer activation curve is shifted to more positive displacements. The current–displacement relationships in Fig. 2*D* and in subsequent figures have been fitted with a double-Boltzmann function representing a three-state

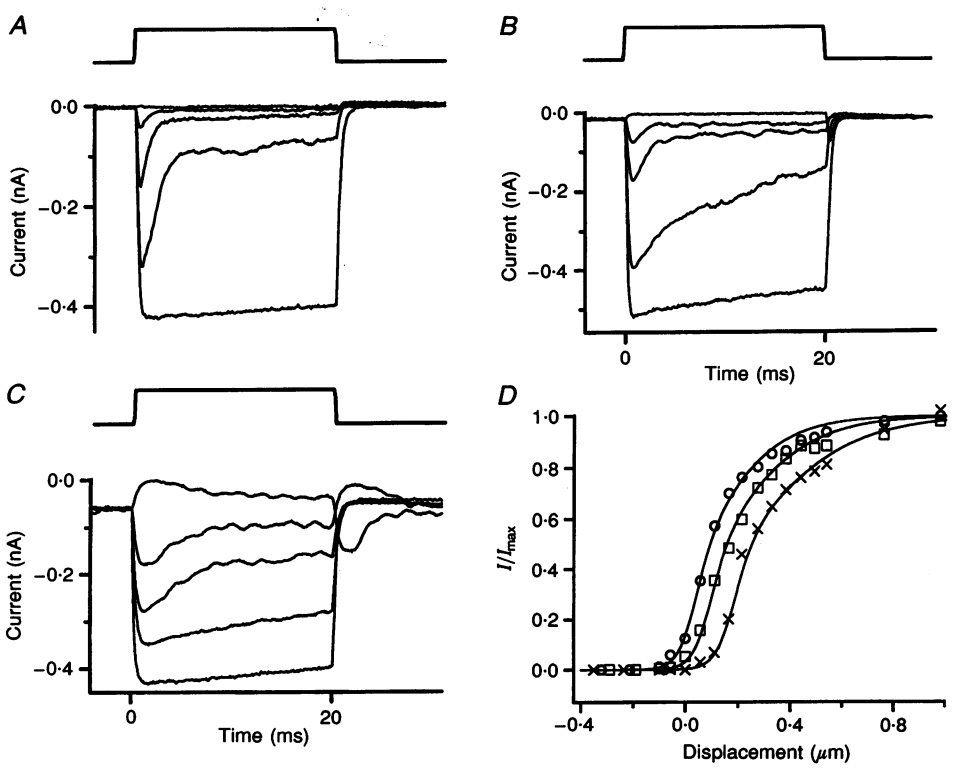

Figure 2. Transducer currents with intracellular BAPTA concentrations of 0·1, 1 and 3 mM

Averaged currents for step deflections of the hair bundle in 3 different cells. *A*, 0·1 mM BAPTA; displacements in nm: −179, 36, 163, 339 and 1000. *B*, 1 mM BAPTA; displacements in nm: −213, 57, 164, 274 and 1000; *C*, 3 mM BAPTA; displacements in nm: −213, 57, 111, 164 and 1000. In this and subsequent figures, positive stimuli are displacements towards the kinocilium evoking an increase in inward current. Zero on the ordinate corresponds to the level at which the transducer current is turned off. Traces are the means of 5–25 responses; holding potential, −70 mV. In each panel, the top trace gives the timing of the 20 ms voltage step delivered to the bimorph. *D*, response–displacement relationships derived from currents in *A*–*C*; the ordinate is the peak current scaled to its maximum value with the largest step (I/I_{max}). Maximum currents and BAPTA concentrations are, respectively: ×, 0·42 nA, 0·1 mM; □, 0·52 nA, 1 mM; ○, 0·42 nA, 3 mM. Smooth curves are double-Boltzmann fits calculated from eqn (1) with: $a_1 = 24\ \mu m^{-1}$, $a_2 = 5\ \mu m^{-1}$, $x_1 = x_2 = 0{\cdot}2\ \mu m$ (×); $a_1 = 24\ \mu m^{-1}$, $a_2 = 6\ \mu m^{-1}$, $x_1 = x_2 = 0{\cdot}11\ \mu m$ (□); $a_1 = 24\ \mu m^{-1}$, $a_2 = 7\ \mu m^{-1}$, $x_1 = x_2 = 0{\cdot}05\ \mu m$ (○). For explanation, see text.

channel with both transitions sensitive to displacement x (Holton & Hudspeth, 1986; Crawford *et al.* 1989):

$$I/I_{max} = (1 + K_2(1 + K_1))^{-1}. \quad (1)$$

K_1 and K_2 are equilibrium constants for the first and second transitions with:

$$K_1 = \exp(a_1(x_1 - x)),$$

and

$$K_2 = \exp(a_2(x_2 - x)),$$

where a_1, a_2, x_1 and x_2 are constants determining the steepness of the function and its position along the displacement axis, respectively.

The adaptation time constant was measured from single exponential fits which in the majority of cases adequately described the major portion of the current decline (Fig. 3*C* and *D*). There was also a slower component to adaptation (Crawford *et al.* 1989) which was not quantified due to its small amplitude. Such fits were applied to currents evoked by small step displacements of the hair bundle producing less than a half-maximal response. Both the mean time constant and extent of adaptation changed systematically with the BAPTA concentration (Fig. 3*A*). Moreover, when the results from different BAPTA concentrations were pooled, the rate and extent of adaptation were correlated (Fig. 3*B*). Measurements in 2·8 mM and 50 μM Ca^{2+} endolymph overlapped and when the two sets of data in

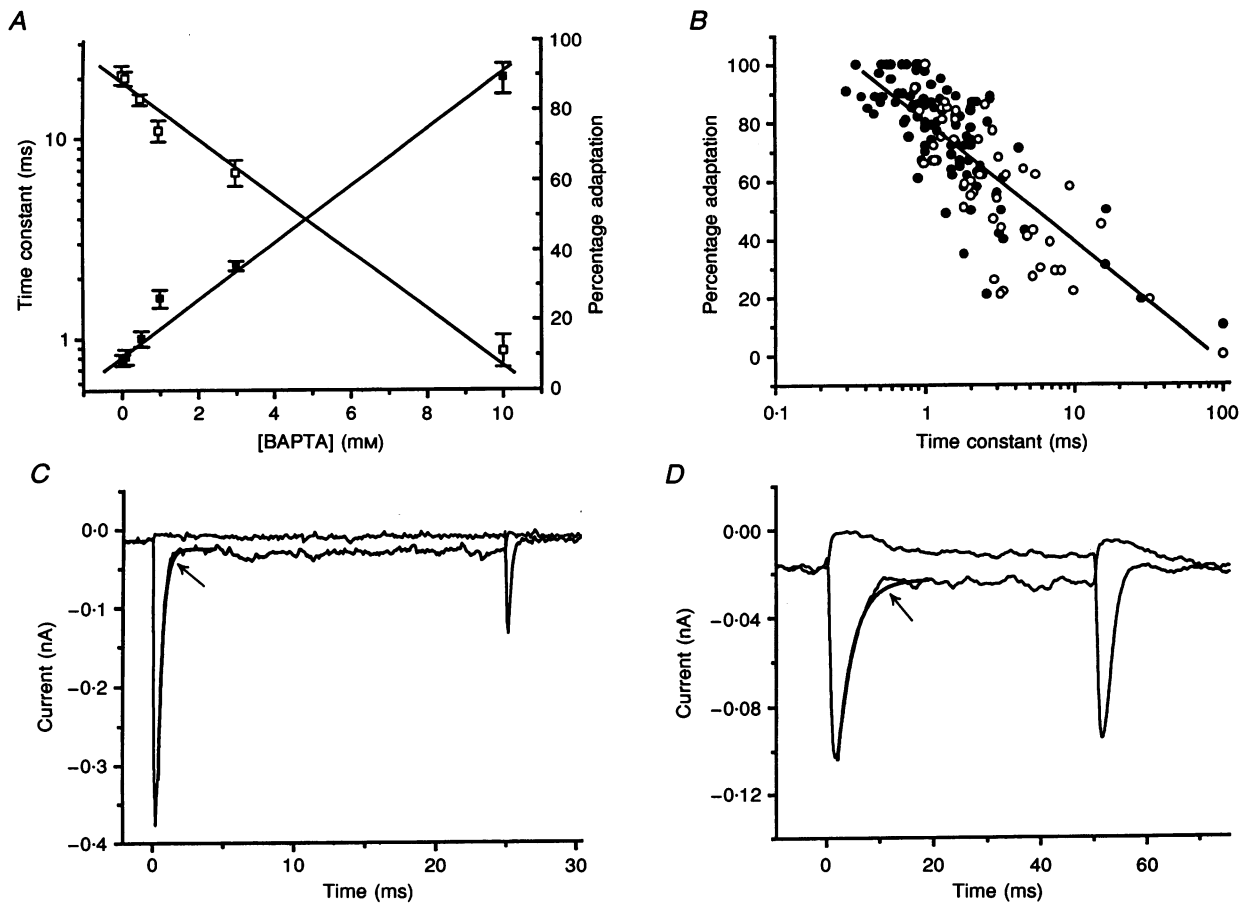

Figure 3. Effects of BAPTA concentration on time constant and extent of adaptation

A, collected means (± 1 S.E.M.) of time constants (■, left-hand ordinate) and percentage adaptation, the reduction in the current relative to the total current (□, right-hand ordinate). BAPTA concentrations and number of values, respectively, averaged: 0·01 mM, 9; 0·1 mM, 22; 0·5 mM, 25; 1 mM, 28; 3 mM, 16; 10 mM, 3. The means do not include an additional 6 cells in 3 mM BAPTA and 6 cells in 10 mM BAPTA with no adaptation for a 50 ms stimulus. Lines are regression fits; $r = 0{\cdot}97$ for the time constant and −0·99 for the degree of adaptation. *B*, individual measurements of percentage adaptation against time constant for endolymphs containing 2·8 mM Ca^{2+} (●) and 50 μM Ca^{2+} (○). Line is regression fit to all points; $r = -0{\cdot}88$. *C*, averages of 25 responses to small (± 150 nm) stimuli for internal [BAPTA] of 0·1 mM. *D*, averages of 25 responses to small (± 50 nm) stimuli for internal [BAPTA] of 1 mM. Thick lines in *C* and *D* (arrows) show exponential fits to current decay; time constant (τ), 0·3 ms in *C* and 2·8 ms in *D*. Holding potential, −70 mV. Uncompensated series resistance, 120 μs (*C*) and 160 μs (*D*).

Fig. 3*B* were fitted separately they had similar regression slopes (●, $-38\ ms^{-1}$, $r = 0{\cdot}76$; ○, $-41\ ms^{-1}$, $r = 0{\cdot}88$). These plots are consistent with the rate and extent of adaptation being co-regulated by the intracellular free Ca^{2+} concentration: with lower [BAPTA], a larger fraction of the Ca^{2+} entering the stereocilia would remain free.

There was some variability in the characteristics of adaptation in different cells depending on the size of the current. For example in 3 and 10 mM BAPTA, adaptation disappeared in a proportion of cells that had smaller than average currents. This set of cells are not included in the mean values plotted in Fig. 3*A* so the effects of the higher BAPTA concentrations will be underestimated by the mean values. In contrast, for some recordings in the lowest [BAPTA], the current adapted completely with a time constant as fast as 0·3 ms (Fig. 3*B* and *C*). It seems unlikely that such fast time constants result artifactually from the probe becoming detached from the bundle since similar fast responses were visible at the end of a negative step (Fig. 3*C* and *D*). The fastest time constants are scarcely different from the time constant of deactivation of the current at the end of the step which reflects channel closure. This argues that the sequence of events triggered on Ca^{2+} entry occur on a time scale of a fraction of a millisecond.

Variations in transduction with hair cell location

The transducer currents measured in the intact papilla were severalfold larger than in isolated cells, suggesting that more channels were functional. The peak amplitude of the current depended on the location of the hair cell in the papilla, the largest values measured at a given position increasing from about 200 pA at the low-frequency end near the lagena to more than 600 pA towards the high-frequency end. This variation may be partly explained by a concurrent increase in the number of stereocilia per bundle along the papilla (~60 at the apex increasing to ~90 at the base; Hackney *et al.* 1993). On perfusing 50 μM Ca^{2+} endolymph, the

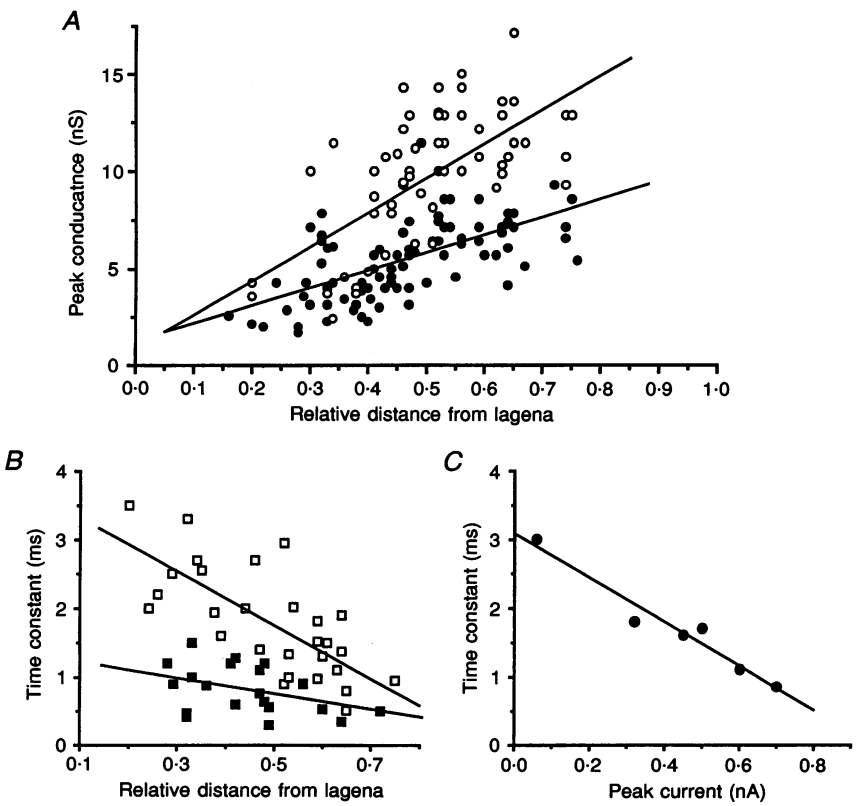

Figure 4. Variation of transducer conductance and adaptation time constant with hair cell location

A, maximum conductance plotted against relative distance of the hair cell along the basilar papilla for 88 cells in 2·8 mM Ca^{2+} endolymph (●) and for 83 cells in 50 μM Ca^{2+} (○). For each measurement, the distance of the cell from the lagenar (low-frequency) end of the papilla was normalized to the total length of the cochlea (~830 μm). Measurements include all internal [BAPTA] from 0·01 to 1 mM. Lines are fits with slope and regression coefficients: 9 nS, $r = 0{\cdot}61$ (●) and 18 nS, $r = 0{\cdot}65$ (○). *B*, fast time constant of adaptation plotted against relative distance of the hair cell along the basilar papilla for 28 cells with 1 mM intracellular BAPTA (□) and 20 cells with 0·1 mM intracellular BAPTA (■). Lines are regression fits, $r = -0{\cdot}74$ (□) and $-0{\cdot}4$ (■). *C*, for a fixed cochlear location, the adaptation time constant is plotted against the peak transducer current for 6 cells recorded with 3 mM intracellular BAPTA. Measurements were derived from cells at fractional distances from lagena of between 0·51 and 0·67. Line is regression fit, $r = -0{\cdot}97$.

maximum currents in cells throughout the cochlea were amplified about 2-fold, but the gradient in the maximum current was still evident. Linear regression fits have been superimposed on the data in Fig. 4*A* to show the correlation between maximum conductance and hair cell position. However, if the scatter in the results is due to variable damage to the hair bundles during dissection, then the upper envelopes of the sets of points are more likely to approximate the physiological condition.

The maximum currents translate into a conductance range of approximately 2·5–9 nS in endolymph containing 2·8 mM Ca^{2+} and 4–17 nS in 50 μM Ca^{2+} (Fig. 4*A*). Taking into account the variations in ciliary complement, the total conductance corresponds to 40–100 pS per stereocilium in 2·8 mM Ca^{2+} and 70–190 pS per stereocilium in 50 μM Ca^{2+}. The maximum conductance of approximately 17 nS in 50 μM Ca^{2+} endolymph is still smaller than the value of 25 nS estimated for hair cells in the intact cochlea (Fettiplace, 1992). One factor that may contribute to this discrepancy is the identity of the monovalent cation: Na^+ in the present experiments but K^+ in the intact cochlea. Substitution of K^+ for Na^+ has previously been shown to produce a 36% increase in the current magnitude (see Table 2 of Crawford *et al.* 1991).

There was a proportional decrease in the time constant of adaptation with hair cell location, which is illustrated in Fig. 4*B* for two different internal BAPTA concentrations (0·1 and 1 mM). For each intracellular [BAPTA], there was an approximately 4-fold change along the papilla but recordings with the lower [BAPTA] gave shorter overall time constants. For both buffer concentrations, the fastest adaptation time constants occurred in cells at the base, which will be tuned to high frequencies. The correlation between time constant and hair cell location raises the possibility that adaptation may play a role in hair cell frequency tuning.

It is possible that the change in time constant with hair cell location results at least partly from the change in peak conductance. In support of this notion it was found that, even at one cochlear position, experimental variations in the size of the transducer conductance were associated with concurrent changes in the speed of adaptation. This relationship is illustrated in Fig. 4*C* for cells with a range of conductances, presumably stemming from variable damage during isolation. It was also found that the reduction in current magnitude due to treatment with streptomycin was associated with a slowing of the adaptation time constant. Thus in one cell where the peak current was halved in

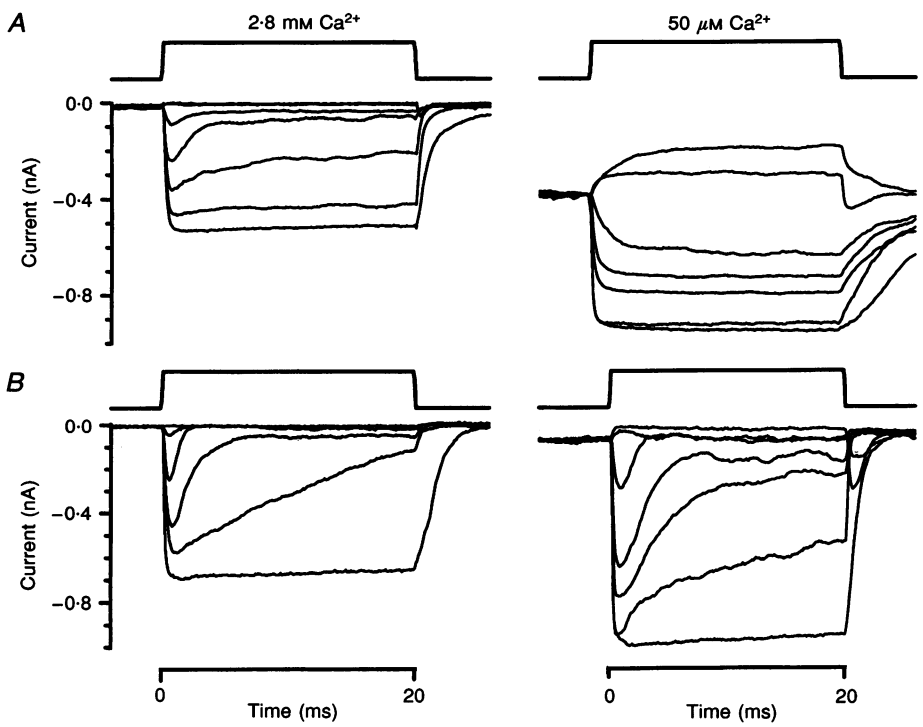

Figure 5. Effects of 50 μM Ca^{2+} endolymph with different internal BAPTA concentrations

A, 1 mM BAPTA. Endolymph Ca^{2+} and displacements in nm: left, 2·8 mM Ca^{2+}; −47, −192, 51, 150, 295, 537 and 1070; right, 50 μM Ca^{2+}; −47, −192, 51, 110, 439, 537 and 975. *B*, 0·01 mM BAPTA. Endolymph Ca^{2+} and displacements in nm: left, 2·8 mM Ca^{2+} ; −47, −192, 51, 150, 243, 387, 487 and 1070; right, 50 μM Ca^{2+}; −47, −192, 51, 295, 387, 679 and 1070. Each trace is the mean of 5–25 responses; holding potential, −70 mV. Top traces show timing of the voltage step to the piezoelectric stimulator. Both cells were from the mid-frequency region of the papilla.

streptomycin, the adaptation time constant increased from 2·4 to 4·1 ms.

Adaptation in low-Ca^{2+} endolymph

When the endolymph Ca^{2+} was reduced from 2·8 mM to 50 μM (with no Mg^{2+}), the fraction of the conductance on at rest increased (Crawford *et al.* 1991), manifesting itself as a leak conductance. The leak conductance could be turned off by negative displacement of the hair bundle or by perfusion with 0·1 mM dihydrostreptomycin, which in low Ca^{2+} totally blocks the transducer channels (Kroese, Das & Hudspeth, 1986). The effects of 50 μM Ca^{2+} endolymph also depended on the intracellular Ca^{2+} buffering (Fig. 5). With high buffering (Fig. 5*A*), there was an increase in the maximum size of the current and the proportion activated at rest, as well as a loss of adaptation. With low buffering (Fig. 5*B*), the maximum size of the current and the proportion activated at rest increased but adaptation remained. In the example shown, both the time constant (0·9 ms) and the extent of adaptation (100%) were little changed in 50 μM Ca^{2+}. With low Ca^{2+} the time constant increased to 1 ms but the degree of adaptation was 100% for small-amplitude stimuli. The difference is a quantitative one since for both cells illustrated there was a leftward shift in the current–displacement relationship (Fig. 6*A* and *B*) but the net result was that for the lower buffer a smaller fraction of the total current was activated at rest.

In studying the effects of BAPTA, variability in behaviour was observed and only a fraction of the cells retained adaptation in 50 μM Ca^{2+} endolymph; this fraction decreased with BAPTA concentration (Fig. 7*A*). For example, with 0·01 mM BAPTA, five out of six cells retained fast adaptation of mean time constant, 2·2 ± 0·4 ms, with the current declining to 26% of its peak value; in 1 mM BAPTA, about a third of the cells (6 out of 17) retained adaptation and in those cells the mean time constant increased to 3·1 ± 0·5 ms with the current declining to only 50% of its peak value. In 3 mM BAPTA only one cell of seven showed adaptation with a time constant of 8·1 ms. The variability in loss of adaptation in low-Ca^{2+} endolymph was partly related to the location of the hair cell (Fig. 7*B*). Thus all six cells preserving adaptation in 1 mM BAPTA were near the high-frequency end of the cochlea at distances from the lagena more than 0·5 of the total length of the basilar membrane. In contrast, the majority of cells from the low-frequency half of the papilla displayed adaptation in 50 μM Ca^{2+} endolymph only if the [BAPTA] was 0·1 mM or less.

When 250 μM Ca^{2+} endolymph was perfused, intermediate effects were observed. Thus fast adaptation was preserved in almost all cells irrespective of position with 1 mM BAPTA or less, though in the higher buffer concentrations the time constant was slowed up to 2-fold. A question of physiological relevance is whether the variation in time constant with location along the basilar membrane seen in 2·8 mM Ca^{2+} (Fig. 4*B*) was preserved when the endolymphatic Ca^{2+} was reduced to 50 μM. Although less complete results were available, there was a suggestion that, for cells recorded with 0·01 or 0·1 mM BAPTA, the adaptation time constant (range, 0·9–7 ms) was still graded with the position of the hair cell, with the fastest time constants in the basal high-frequency cells.

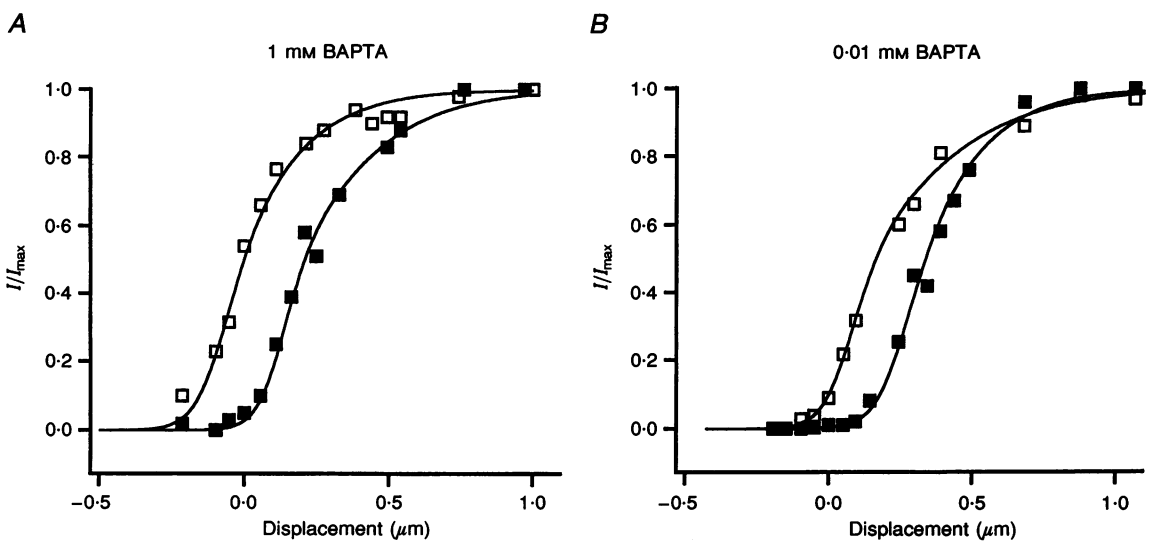

Figure 6. Current–displacement relationships in 2·8 mM and 50 μM Ca^{2+}

Transducer currents scaled to their maximum values are plotted against displacement for 2·8 mM Ca^{2+} (■) and 50 μM Ca^{2+} (□) for cells of Fig. 5; 1 mM internal [BAPTA] (*A*) and 0·01 mM BAPTA (*B*). Smooth curves have been calculated from eqn (1): *A*, $a_1 = 18\ \mu m^{-1}$, $a_2 = 5\ \mu m^{-1}$, $x_1 = x_2 = 0{\cdot}15\ \mu m$, $I_{max} = 0{\cdot}52$ nA (■); $a_1 = 15\ \mu m^{-1}$, $a_2 = 6\ \mu m^{-1}$, $x_1 = x_2 = -0{\cdot}06\ \mu m$, $I_{max} = 0{\cdot}90$ nA (□); *B*, $a_1 = 15\ \mu m^{-1}$, $a_2 = 6{\cdot}5\ \mu m^{-1}$, $x_1 = x_2 = 0{\cdot}16\ \mu m$, $I_{max} = 0{\cdot}70$ nA (■); $a_1 = 18\ \mu m^{-1}$, $a_2 = 4{\cdot}5\ \mu m^{-1}$, $x_1 = x_2 = -0{\cdot}01\ \mu m$, $I_{max} = 0{\cdot}96$ nA (□).

The set position of the transducer

An important characteristic for the proper functioning of the hair cells is the 'set point' of the transducer, which is the fraction of the total transducer conductance activated at the resting position of the bundle. If this fraction is too large, the sensitivity and dynamic range of transduction will be diminished and if it is too small, low-intensity stimuli will fail to evoke a response. The fraction has been estimated as about 0·1 for hair cells in the intact turtle cochlea (Crawford & Fettiplace, 1981*b*).

The position of the current–displacement relationship was quantified by measuring as a function of [BAPTA] the bundle displacement for half-activation of the maximum current ($x_{0.5}$) and the fraction of total current turned on at rest (Fig. 7*C* and *D*). In high Ca^{2+} (2·8 mM) endolymph, no more than 10% of the conductance was activated at rest, this fraction being smaller the lower the Ca^{2+} buffer concentration (Fig. 7*D*). The buffer had a small effect on the position of the current–displacement relationship in normal Ca^{2+}, but in low Ca^{2+} larger changes were observed. For example, the mean leftward shift produced by 50 μM Ca^{2+} endolymph was 100 nm in 0·01 mM BAPTA compared with 250 nm in 3 mM BAPTA. Also the fraction of current activated at rest increased from a mean value of 0·25 with 0·01 mM BAPTA to 0·55 with 3 mM BAPTA. There were no major changes in sensitivity in low compared with normal Ca^{2+} endolymph. When the transducer current was normalized to its peak value and plotted *versus* displacement (see Fig. 6), the maximum slopes in 2·8 mM and 50 μM Ca^{2+} were $4{\cdot}1 \pm 0{\cdot}6$ and $3{\cdot}4 \pm 0{\cdot}4\ \mu m^{-1}$, respectively (0·1 mM BAPTA intracellular; $n = 7$) and

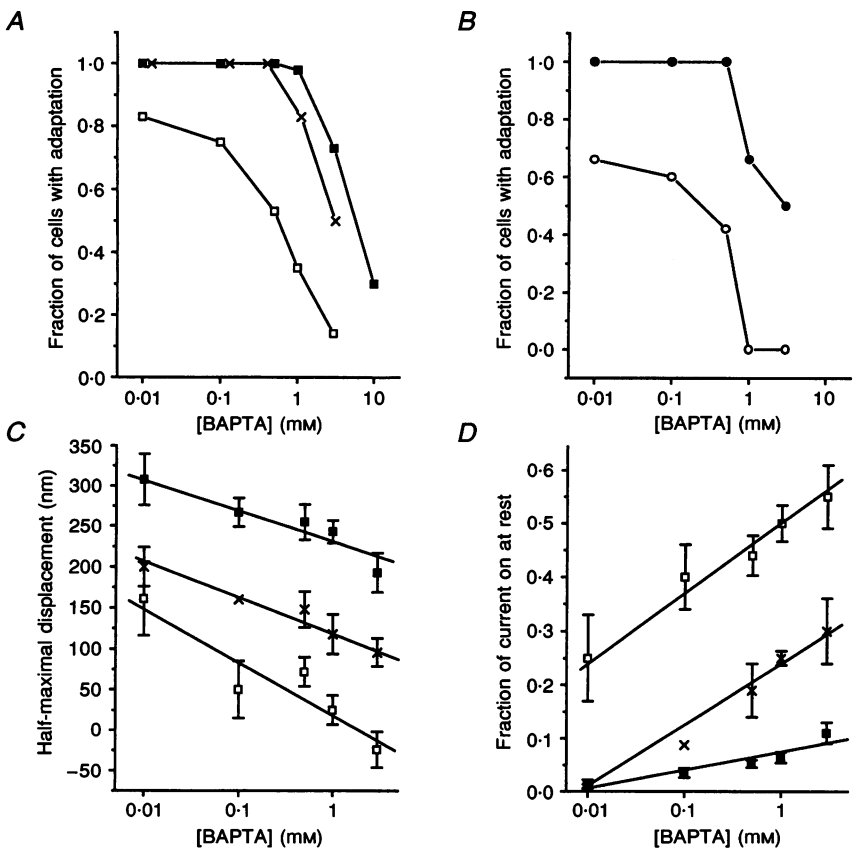

Figure 7. Effects of internal BAPTA concentration on transducer activation curves in high- and low-Ca^{2+} endolymph

A, fraction of cells which displayed adaptation *versus* BAPTA concentration. Different symbols in each plot correspond to different endolymph Ca^{2+} concentrations: 2·8 mM (■), 250 μM (×), 50 μM (□). Cells pooled from the entire papilla. *B*, fraction of cells displaying adaptation in 50 μM Ca^{2+} *versus* BAPTA concentration. Different plots are from cells in two halves of the papilla: ●, recordings from the basal high-frequency half of the papilla; ○, recordings from the apical low-frequency half. Each point corresponds to between 2 and 12 cells. *C*, half-maximal displacement plotted against BAPTA concentration; pooled values for entire papilla. *D*, fraction of transducer current activated at rest plotted against BAPTA concentration; each point is the mean ± 1 S.E.M. of between 6 and 32 values for the control and 50 μM Ca^{2+}; for some measurements with 250 μM Ca^{2+}, fewer values were averaged. Endolymph Ca^{2+} concentrations in *C* and *D*: 2·8 mM (■), 250 μM (×); 50 μM (□). Straight lines drawn by eye.

4·2 ± 0·2 and 2·9 ± 0·3 μm^{-1}, respectively (1 mM BAPTA intracellular; $n = 15$). The slope factors in 2·8 mM Ca^{2+} are not substantially different from those obtained previously in isolated hair cells (see Fig. 2 of Crawford *et al.* 1989).

Several observations suggested that the effects of switching to 50 μM Ca^{2+} endolymph were partly intracellular. Firstly, the shift in the current–displacement relationship was progressive and developed with a time course that was slower than that of the solution change. Secondly, on returning to 2·8 mM Ca^{2+} the current–displacement relationship shifted back but overshot its original position. A transient decrease in the time constant and increase in extent of adaptation accompanied this overshoot. These observations would be consistent with a slow change in the internal Ca^{2+} concentration on changing between the two different endolymph solutions. Thirdly, there was some variability in the augmentation of the maximum current in low Ca^{2+}, ranging between 1·5- and 3-fold. Explanations of the current amplification revolve around relief of Ca^{2+} block of the channel (Crawford *et al.* 1991) by analogy with the Ca^{2+} block described for the cGMP-gated channel in photoreceptors (Zimmerman & Baylor, 1992). However, in photoreceptors, block by divalent cations can occur at both the internal and external surfaces of the channel. It is conceivable that the mechano-electrical transducer channel also experiences block at both the internal and external surfaces, and that the variable relief of block in 50 μM Ca^{2+} reflects a variability in the initial Ca^{2+} concentration at the intracellular mouth of the channel.

cAMP analogues

While the Ca^{2+} buffering within the stereocilia is an important factor governing adaptation, other factors may contribute to the optimal positioning of the activation curve. One such factor is cAMP, whose synthetic enzyme has been reported in the hair bundle (Oudar *et al.* 1990; Drescher *et al.* 1995). The effects of cAMP agonists on the transducer currents and current–displacement relationship are shown in Figs 8 and 9. For these experiments relatively long recording times were needed during which period the control half-saturating displacement ($x_{0.5}$) remained stable. For example, in Fig. 9*A*, the control $x_{0.5}$ lay in the range 300–400 nm. $x_{0.5}$ was shifted negative in 50 μM Ca^{2+} endolymph, and then on return to normal saline there was a transient overshoot before returning to the control range. Perfusion with 0·1 mM of the cAMP agonist 8-Br-cAMP over the course of 5 min produced a substantial shift in the opposite direction. In six such experiments (1 mM BAPTA, intracellular), the positive shift in 8-Br-cAMP ranged from 140 to 473 nm with a mean of 260 ± 49 nm. Similar effects were seen with the phosphodiesterase inhibitor IBMX, which at a concentration of 0·5 mM produced a mean positive shift of 258 ± 34 nm ($n = 4$). The action of IBMX argues that a basal level of cAMP exists in the hair cells, implying that the synthetic pathway for the intracellular messenger must be constitutively active.

Besides their effects on transduction, 8-Br-cAMP and IBMX both produced an augmentation of the voltage-dependent Ca^{2+} current which was reversible on removal of

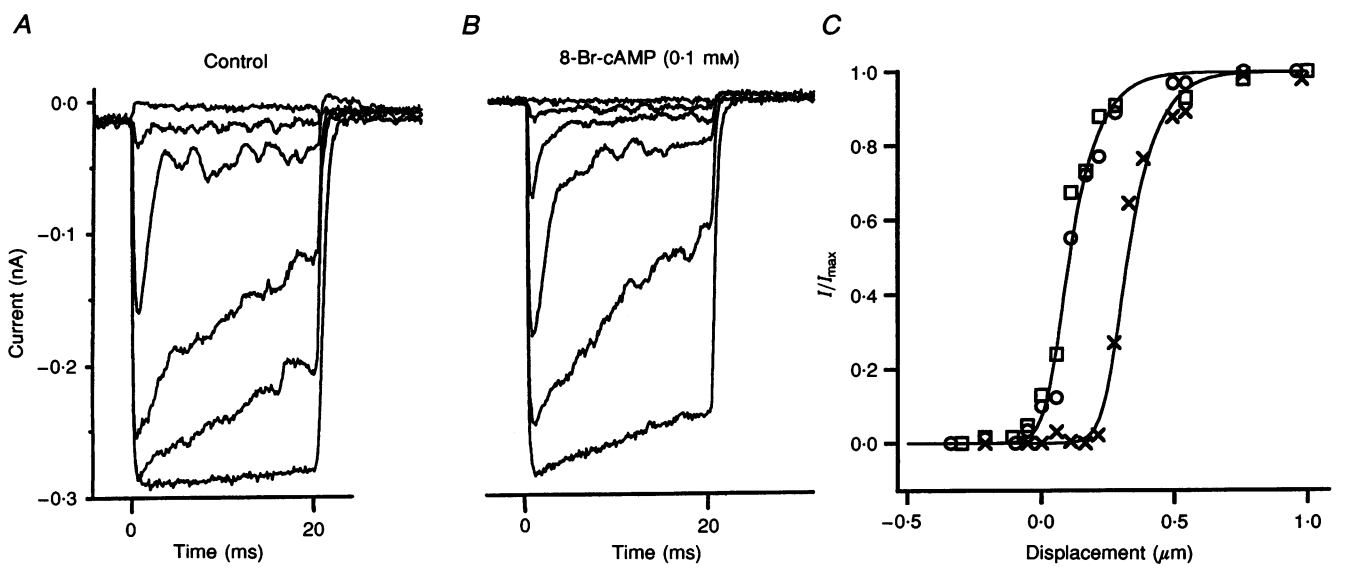

Figure 8. Effects of 8-bromo-cAMP on transducer currents

A, control currents for displacement steps of −213, 57, 213, 381, 491 and 980 nm. *B*, currents after 5 min perfusion of 0·1 mM 8-Br-cAMP to the endolymphatic surface for displacement steps of −213, 57, 213, 327, 491 and 980 nm. *C*, current normalized to its maximum value plotted against displacement for control (□), 8-Br-cAMP (×) and wash (○). Internal BAPTA concentration, 1 mM. Smooth curves have been calculated from eqn (1) with $a_1 = 21\ \mu m^{-1}$, $a_2 = 12\ \mu m^{-1}$, $x_1 = x_2 = 0{\cdot}07\ \mu m$ (Control), and $a_1 = 21\ \mu m^{-1}$, $a_2 = 12\ \mu m^{-1}$, $x_1 = x_2 = 0{\cdot}29\ \mu m$ (8-Br-cAMP).

the agonist (mean fractional increase, 0·27 ± 0·05, $n = 11$). The increase in Ca^{2+} current occurred without any shift in its voltage sensitivity, and may explain the potentiation of vestibular nerve firing with cAMP agonists reported by Ricci *et al.* (1991). One hypothesis for the effect of cAMP on transduction is that it acts by changing intracellular Ca^{2+}, but several observations argue against such a hypothesis. Firstly, in the present experiments a resting Ca^{2+} influx should not occur through voltage-dependent channels since the hair cells were held at −70 mV where the Ca^{2+} current would not be activated. Secondly, the presence or absence of the cAMP analogue did not affect the shift in $x_{0.5}$ produced in low-Ca^{2+} endolymph (Fig. 9). Thus the initial shift on switching from control solution was −274 ± 46 nm and on changing from cAMP analogue in normal endolymph to the analogue in low Ca^{2+} it was −328 ± 48 nm ($n = 5$). These results suggest that the intracellular effects of low Ca^{2+} and cAMP sum independently. It is worth noting that, in Fig. 9, the combined effects of 8-Br-cAMP or IBMX countered the leftward shift in low Ca^{2+}, $x_{0.5}$ assuming a value similar to that in high (2·8 mM) Ca^{2+} endolymph. Thirdly the effect of 0·1 mM 8-Br-cAMP was insensitive to the amount of intracellular Ca^{2+} buffer. The positive shift in $x_{0.5}$ in 0·01 mM BAPTA was 238 ± 86 nm ($n = 3$) and in 3 mM BAPTA was 160 nm ($n = 1$) compared with the 1 mM BAPTA value of 260 ± 49 nm. Finally, the shift in $x_{0.5}$ occurred without any change in the time course or extent of adaptation (Fig. 8). Taken together these observations argue that cAMP has a separate action from intracellular Ca^{2+} and suggest that, under some conditions, the position of the activation curve can be dissociated from the presence of adaptation to a step stimulus.

DISCUSSION

Adaptation and the optimal position of the transducer activation curve

Adaptation of the transducer channels of the hair cells, triggered by Ca^{2+} influx, is thought to optimize the sensitivity of the transducer near the resting position of the hair bundle (Eatock *et al.* 1987). Paradoxically, the hair cells are arranged with the transducing apparatus enveloped in endolymph containing a Ca^{2+} concentration of less than 100 μM. Exposure of isolated hair cells to such Ca^{2+} levels has been shown to abolish adaptation and turn on a substantial fraction of the transducer current at rest (Crawford *et al.* 1991). To address this paradox, we have examined the contribution of intracellular Ca^{2+} buffering to transduction in an intact cochlear epithelium where the endolymphatic surface could be perfused with low-Ca^{2+} solution. We found that fast adaptation is retained in 250 or 50 μM endolymphatic Ca^{2+} provided the cell contains a

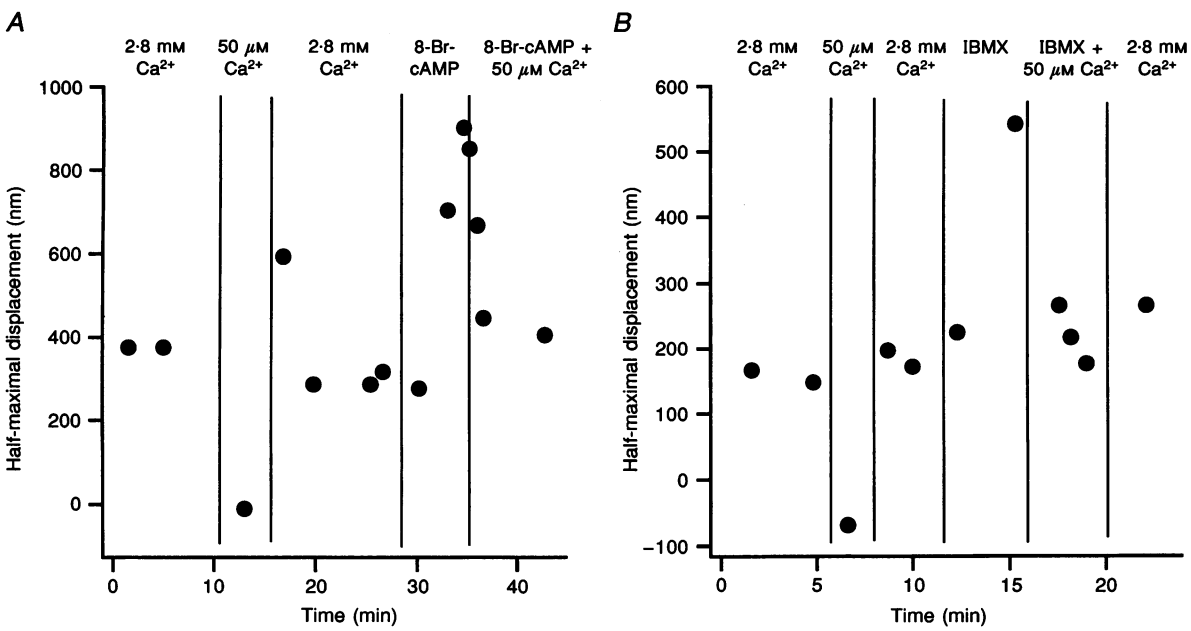

Figure 9. Effects of 8-bromo-cAMP and IBMX on position of transducer activation curve

A, changes in $x_{0.5}$, the displacement to produce half-activation of the transducer current during perfusion of endolymph containing 2·8 mM Ca^{2+}, 50 μM Ca^{2+} or 2·8 mM Ca^{2+} plus 0·1 mM 8-Br-cAMP, as indicated at the top; in between, control solution containing 2·8 mM Ca^{2+} was continuously delivered. *B*, changes in half-maximal displacement ($x_{0.5}$) in another cell during perfusion of 50 μM Ca^{2+} or 0·5 mM IBMX. Internal BAPTA concentration, 1 mM. The $x_{0.5}$ values were measured from families of displacement steps delivered at a low rate every few minutes so as not to degrade the transducer properties during a long recording. Zero time on the abscissae corresponds to the point at which the cell properties stabilized, which was about 10 min after breakthrough.

sufficiently low concentration of Ca^{2+} buffer. Preservation of adaptation in low-Ca^{2+} solution is also more likely in cells with large maximal responses. Taken together, these observations suggest that the rate and extent of adaptation are determined by the Ca^{2+} influx and the stereociliary buffering capacity.

Our results also indicated that the position of the current–displacement curve depended on the internal Ca^{2+} buffer concentration (Fig. 7), but even in the lowest BAPTA concentrations, 25% or more of the transducer conductance was activated at rest in 50 μM endolymphatic Ca^{2+}. This observation differs from the measurements in the intact cochlea where no more than 10% of the transducer conductance is activated at rest (Fettiplace, 1992). While the Ca^{2+} buffer concentration is clearly important in setting the position of the current–displacement curve, additional factors must be involved in the intact organ. One factor may be the cyclic nucleotide concentration.

The relationship between transducer conductance and time constant of adaptation

The results in Fig. 4 suggest that cells with a larger transducer conductance exhibit faster adaptation. The simplest explanation for this correlation is that a larger conductance results in a greater Ca^{2+} influx. Consequently, the divalent ion achieves a higher stereociliary concentration and drives adaptation more rapidly. Consistent with this notion, when the endolymph Ca^{2+} was reduced to 50 μM, adaptation in high-frequency cells with larger transducer conductances was more resistant to internal [BAPTA] (Fig. 7*B*). For such a mechanism to operate, there needs to be intracellular summation of Ca^{2+} entering through different channels, assuming that the conductance and Ca^{2+} permeability of the channel remain the same in all hair cells. The transducer channels are thought to be located at the stereociliary tips (Jaramillo & Hudspeth, 1991; Lumpkin & Hudspeth, 1995; Denk *et al.* 1995); therefore, due to the long diffusion distances, interaction between channels in neighbouring stereocilia would be unlikely to occur on a time scale fast enough to affect adaptation. Local summation would be more likely if each stereocilium contained multiple channels within a short diffusional distance of each other. Summation from channels at either end of the tip link (Denk *et al.* 1995) may be one explanation. Alternatively, in high-frequency hair cells, one end of the tip link may be attached to multiple channels.

Derivation of the number of channels per stereocilium is not straightforward given the spread in the single-channel estimates (50 pS, Ohmori, 1985; 17 pS, Holton & Hudspeth, 1986; 106 pS, Crawford *et al.* 1991). The lowest value was obtained by measurements of current noise and the two larger values from observation of discrete channel events. The spread might be reconciled if it is assumed that the channels can exhibit fast flicker block like the cyclic nucleotide-gated channel of the photoreceptors (e.g. Torre, Strafforini, Sesti & Lamb, 1992) and so their 'effective' amplitude estimated by noise measurements especially in high Ca^{2+}, would be smaller than the closed-to-open amplitude of discrete current events. Using Holton & Hudspeth's (1986) value of 17 pS and a conductance range along the papilla of 40–100 pS per stereocilium in 2·8 mM Ca^{2+}, this gives 2·5–6 channels per stereocilium. Although the discrete channel events were observed in cells bathed in high Ca^{2+}, it is more appropriate to relate their size to the total conductance measured in 50 μM Ca^{2+}, where flicker block of the channels might be minimized. Using the channel amplitudes of Ohmori (1985) and of Crawford *et al.* (1991) and a conductance range in 50 μM Ca^{2+} of 70–190 pS per stereocilium gives 1·5–3·8 and 0·7–1·9 channels per stereocilium, respectively. The increase in the transducer conductance with position along the turtle cochlea may thus be achieved by increases in both the number of stereocilia and the number of channels per stereocilium. However, the different values of unitary conductance all imply only a small number of channels per stereocilium even in high-frequency cells. Whether these numbers are sufficient to provide the requisite Ca^{2+} summation in order to account for the change in adaptation time constant is uncertain. More detailed information about the single transducer-channel properties might help to clarify the problem

The systematic variation in adaptation time constant with cochlear location (Fig. 4*B*) suggests that it might play a physiological role. If adaptation operates in the intact cochlea, it will contribute a high-pass filter to the frequency selectivity of the hair cell. Original attempts to dissect the cell's acoustic tuning curve in the turtle cochlea (Crawford & Fettiplace, 1981*a*) indicated that, besides the major component endowed by the electrical resonance, there was a residual low-pass filter (the middle ear mechanics) and a single-pole high-pass filter of unknown origin. The high-pass filter varied from 29 to 350 Hz and was roughly scaled with the characteristic frequency of the hair cell (see Table 4 of Crawford & Fettiplace, 1981*a*). A variation in the time constant of transducer adaptation could account for this filter especially since the absolute range is approximately correct. For example, time constants between 0·5 and 2 ms (Fig. 3*B*) are equivalent to 3 dB corner frequencies from 320 to 80 Hz, respectively. The time constants were increased in low Ca^{2+} to between 0·9 and 7 ms (0·01 or 0·1 mM BAPTA), but the values still span a frequency range of 23–180 Hz.

Calcium buffering in the hair bundle

To allow for proper control of the mechanotransduction apparatus intracellular Ca^{2+} may be regulated in the hair bundle independently of the cell body. This would ensure that its resting concentration is kept low and that local changes in concentration are adequate to modulate transducer channel activity. Extrusion probably occurs via a Ca^{2+}-ATPase (Tucker & Fettiplace, 1995), which has been reported to be highly concentrated in the stereociliary plasma membrane (Crouch & Schulte, 1995). The endogenous Ca^{2+} buffer in the cell body has been estimated to be equivalent to ~1 mM BAPTA from the effects of different

BAPTA concentrations on the Ca^{2+}-activated K^+ currents both in mid-frequency turtle hair cells (Tucker & Fettiplace, 1996) and in bullfrog hair cells (Roberts, 1994). In recordings with 1 mM BAPTA, only about a third of the cells displayed adaptation in 50 μM Ca^{2+} endolymph (Fig. 7*A*), but it is significant that all these cells came from the high-frequency end of the papilla where the transduction currents were larger. For adaptation to persist in low-frequency cells in 50 μM Ca^{2+} endolymph, the BAPTA needed to be 0·1 mM or less. One explanation for this variation is that hair cells closer to the low-frequency end contain less endogenous Ca^{2+} buffer both in their cell body and stereocilia. This would imply a gradient in the Ca^{2+} buffer concentration along the cochlea to accompany the change in magnitude of the transducer conductance. Alternatively the Ca^{2+} buffer concentration in all hair cells is lower in the hair bundle than in the cell body.

For a given internal BAPTA concentration, there was variation between cells both in the characteristics of adaptation and in the response to low-Ca^{2+} endolymph. Variability has been noted by Shepherd & Corey (1994) who found a range of adaptation time constants, though their mean value of 25 ms obtained with 10 mM internal EGTA is in good agreement with our measurements in 10 mM BAPTA. The variability may be due in part to differences in the magnitude of the transducer current or location of the hair cell (see above). It could also reflect differences in Ca^{2+} loading of the stereocilia, which might arise during the dissection, when the hair bundles are immersed in an unphysiological high-Ca^{2+} environment. Such effects would be exacerbated in cells with large transducer conductances. Furthermore the increased metabolic demand for Ca^{2+} extrusion in large-conductance cells would render them more susceptible *in vivo* to Ca^{2+} overload during hypoxia or overstimulation. Variations in transducer channel density, coupled with alterations in intrinsic Ca^{2+} buffering could be postulated to be the mechanisms by which cells modulate adaptation across end organs. Thus slow, incomplete adaptation may be important in vestibular hair cells that operate at low frequencies and need a sustained transducer response (as with gravity receptors), whereas fast and full adaptation may be a feature of cochlear hair cells in order to enhance their frequency selectivity.

cAMP

Our results provide the first evidence that cAMP may also be involved with regulating the mechano-electrical transducer channels. The effect of the nucleotide, to shift the transducer activation curve to the right, is in the same direction as that produced by an increase in intracellular Ca^{2+}. It could therefore have a physiological role in adjusting the 'set point' of the transducer channels in order to optimize their sensitivity at rest, especially in endolymph containing a physiological Ca^{2+} concentration. We have no evidence about the mechanism of action of cAMP, though in theory this might be through a direct action on the channel or via stimulation of a protein kinase that phosphorylates the channel or its ancillary apparatus. An equally important question is how the levels of the nucleotide are controlled. The effects of IBMX argue that, in the absence of external modulators, there is a constitutive turnover in the cyclic nucleotide. An endogenous control might therefore be via changes in internal Ca^{2+} influencing the metabolic machinery by Ca^{2+}-dependent isozymes of adenyl cyclase or phosphodiesterase. Either pathway would provide a feedback loop linking the levels of the two intracellular messengers. Our discovery of a role for cAMP in hair cell transduction may help account for one of the consequences of a recently described mouse mutation *tubby* (Noben-Trauth, Naggert, North & Nishiza, 1996). *tubby* mice suffer late-onset obesity as well as neurosensory hearing loss and have a mutation in a protein tentatively identified as a phosphodiesterase. Absence of phosphodiesterase in hair cells could lead to an elevation in cAMP concentration which may cause deafness by shifting the transducer activation curve beyond the range of physiological stimuli.

Assad, J. A., Hacohen, N. & Corey, D. P. (1989). Voltage dependence of adaptation and active bundle movements in bullfrog saccular hair cells. *Proceedings of the National Academy of Sciences of the USA* **86**, 2918–2922.

Bosher, S. K. & Warren, R. L. (1978). Very low calcium content of cochlear endolymph, an extracellular fluid. *Nature* **273**, 377–378.

Crawford, A. C., Evans, M. G. & Fettiplace, R. (1989). Activation and adaptation of transducer currents in turtle hair cells. *Journal of Physiology* **419**, 405–434.

Crawford, A. C., Evans, M. G. & Fettiplace, R. (1991). The actions of calcium on the mechano-electrical transducer current of turtle hair cells. *Journal of Physiology* **434**, 369–398.

Crawford, A. C. & Fettiplace, R. (1981*a*). An electrical tuning mechanism in turtle cochlear hair cells. *Journal of Physiology* **312**, 377–412.

Crawford, A. C. & Fettiplace, R. (1981*b*). Non-linearities in the responses of turtle hair cells. *Journal of Physiology* **315**, 317–338.

Crouch, J. J. & Schulte, B. A. (1995). Expression of plasma membrane Ca-ATPase in the adult and developing gerbil cochlea. *Hearing Research* **92**, 112–119.

Denk, W., Holt, J. R., Shepherd, G. M. G. & Corey, D. P. (1995). Calcium imaging of single stereocilia in hair cells: localization of transduction channels at both ends of tip links. *Neuron* **15**, 1311–1321.

Drescher, M. J., Kern, R. C., Hatfield, J. S. & Drescher, D. G. (1995). Cytochemical localization of adenyl cyclase activity within the sensory epithelium of the trout saccule. *Neuroscience Letters* **196**, 145–148.

Eatock, R. A., Corey, D. P. & Hudspeth, A. J. (1987). Adaptation of mechanoelectrical transduction in hair cells of the bullfrog's sacculus. *Journal of Neuroscience* **7**, 2821–2836.

Fettiplace, R. (1992). The role of calcium in hair cell transduction. In *Sensory Transduction*, ed. Corey, D. P. & Roper, S. D. *Society for General Physiologists Series* **47**, 343–356.

Hackney, C. M., Fettiplace, R. & Furness, D. N. (1993). The functional morphology of stereociliary bundles on turtle cochlear hair cells. *Hearing Research* **69**, 163–175.

HOLTON, T. & HUDSPETH, A. J. (1986). The transduction channel of hair cells from the bullfrog characterized by noise analysis. *Journal of Physiology* **375**, 195–227.

JARAMILLO, F. & HUDSPETH, A. J. (1991). Localization of the hair cell's transduction channels at the hair bundle's top by iontophoretic application of a channel blocker. *Neuron* **7**, 409–420.

KIMITSUKI, T. & OHMORI, H. (1992). The effect of caged calcium release on the adaptation of the transduction current in chick hair cells. *Journal of Physiology* **458**, 27–40.

KROESE, A. B. A., DAS, A. & HUDSPETH, A. J. (1986). Blockage of the transduction channels of hair cells in the bullfrog's sacculus by aminoglycoside antibiotics. *Hearing Research* **37**, 203–218.

KROS, C. J., RÜSCH, A. & RICHARDSON, G. P. (1992). Mechano-electrical transducer currents in hair cells of the cultured neonatal mouse. *Proceedings of the Royal Society* B **249**, 185–193.

LUMPKIN, E. A. & HUDSPETH, A. J. (1995). Detection of Ca^{2+} entry through mechanosensitive channels localizes the site of mechanoelectrical transduction in hair cells. *Proceedings of the National Academy of Sciences of the USA* **92**, 10297–10301.

NOBEN-TRAUTH, K., NAGGERT, J. K., NORTH, M. A. & NISHIZA, P. M. (1996). A candidate gene for the mouse mutation *tubby*. *Nature* **380**, 534–538.

OHMORI, H. (1985). Mechano-electrical transduction currents in isolated vestibular hair cells of the chick. *Journal of Physiology* **359**, 189–217.

OLIVA, C., COHEN, I. S. & MATHIAS, R. T. (1988). Calculations of time constants for intracellular diffusion in whole cell patch clamp configuration. *Biophysical Journal* **54**, 791–799.

OUDAR, O., FERRARY, E. & FELDMANN, G. (1990). Adenylate cyclase and carbonic anhydrase in the semicircular canal epithelium of the frog *Rana esculenta*. *Cell and Tissue Research* **262**, 579–585.

PICKLES, J. O., COMIS, S. D. & OSBORNE, M. (1984). Crosslinks between the stereocilia in the guinea pig organ of Corti, and the possible relation to sensory transduction. *Hearing Research* **15**, 103–112.

RICCI, A., NORRIS, C. & GUTH, P. (1991). Cyclic AMP modulates sensory-neural communication in a vestibular end organ. *Brain Research* **565**, 78–84.

ROBERTS, W. M. (1994). Spatial calcium buffering in saccular hair cells. *Nature* **363**, 74–76.

ROBERTS, W. M., JACOBS, R. A. & HUDSPETH, A. J. (1990). Colocalization of ion channels involved in frequency selectivity and synaptic transmission in presynaptic active zones. *Journal of Neuroscience* **10**, 3664–3684.

SHEPHERD, G. M. G. & COREY, D. P. (1994). The extent of adaptation in bullfrog saccular hair cells. *Journal of Neuroscience* **14**, 6217–6229.

TORRE, V., STRAFFORINI, M., SESTI, F. & LAMB, T. D. (1992). Different channel-gating properties of two classes of cyclic GMP-activated channel in vertebrate photoreceptors. *Proceedings of the Royal Society* B **250**, 209–215.

TUCKER, T. & FETTIPLACE, R. (1995). Confocal imaging of calcium microdomains and calcium extrusion in turtle hair cells. *Neuron* **15**, 1323–1335.

TUCKER, T. & FETTIPLACE, R. (1996). Monitoring calcium in hair cells with a calcium-activated potassium channel. *Journal of Physiology* **494**, 613–626.

ZIMMERMAN, A. L. & BAYLOR, D. A. (1992). Cation interactions within the cyclic GMP-activated channel of retinal rods from the tiger salamander. *Journal of Physiology* **449**, 759–783.

Acknowledgements

This work was supported by a research grant (5R01 DC 01362) from the National Institutes on Deafness and Other Communication Disorders, National Institutes of Health. We thank Jon Art for advice and loan of equipment and Mike Wu and Tom Tucker for helpful discussions during the course of the work.

Author's email address

R. Fettiplace: fettiplace@neurophys.wisc.edu

Received 12 November 1996; accepted 25 February 1997.